



## OPEN ACCESS

## EDITED BY

Yi-Chen Ethan Li,  
Feng Chia University, Taiwan

## REVIEWED BY

Tomas Cristian Tempesti,  
CCT CONICET Córdoba, Argentina  
Bahareh Azimi,  
University of Pisa, Italy

## \*CORRESPONDENCE

Zhenzhen Hui,  
✉ qjunanan128@163.com

RECEIVED 28 July 2023

ACCEPTED 01 November 2023

PUBLISHED 01 December 2023

## CITATION

Qiu N, Pan X, Hu R and Hui Z (2023),  
Synthesis of a novel photochemical and  
thermoreponsive diblock biomaterial  
with end-functionalized zinc porphyrin.  
*Front. Bioeng. Biotechnol.* 11:1268458.  
doi: 10.3389/fbioe.2023.1268458

## COPYRIGHT

© 2023 Qiu, Pan, Hu and Hui. This is an  
open-access article distributed under the  
terms of the [Creative Commons  
Attribution License \(CC BY\)](https://creativecommons.org/licenses/by/4.0/). The use,  
distribution or reproduction in other  
forums is permitted, provided the original  
author(s) and the copyright owner(s) are  
credited and that the original publication  
in this journal is cited, in accordance with  
accepted academic practice. No use,  
distribution or reproduction is permitted  
which does not comply with these terms.

# Synthesis of a novel photochemical and thermoresponsive diblock biomaterial with end-functionalized zinc porphyrin

Nannan Qiu<sup>1,2</sup>, Xinyuan Pan<sup>1</sup>, Ruizhang Hu<sup>1,2</sup> and Zhenzhen Hui<sup>1,2\*</sup>

<sup>1</sup>College of Chemistry and Materials Engineering, Anhui Science and Technology University, Bengbu, Anhui, China, <sup>2</sup>Anhui Province Quartz Sand Purification and Photovoltaic Glass Engineering Research Center, Fengyang, Anhui, China

Porphyrin compound-based photochemical molecules and biomaterials have been synthesized for photosensitivity and bioimaging experiments. However, most porphyrin photosensitizers have limited application in biological environments owing to severe aggregation in aqueous solutions. In the present study, we prepared amphipathic and photosensitive copolymers using zinc porphyrin via consecutive atom transfer-free radical polymerizations (ATRPs) comprising photoresponsive and thermosensitive chain segments. Furthermore, we evaluated the photocatalytic activity of the copolymer for methylene blue (MB) in water.

**Methods:** First, we synthesized a photoresponsive chain segment of poly(6-[4-(4-methoxyphenylazo)phenoxy]hexyl methacrylate) (ZnPor-PAzo); then, ZnPor-PAzo was used as a macroinitiator and was polymerized with *N*-isopropylacrylamide (NIPAM) via ATRPs to obtain a novel photochemical and thermoresponsive diblock biomaterial with end-functionalized zinc porphyrin [(ZnPor-PAzo)-PNIPAMs].

**Results:** The polydispersity index ( $M_w/M_n$ ) of (ZnPor-PAzo)-PNIPAMs was 1.19–1.32. Furthermore, its photoresponsive and thermosensitive characteristics were comprehensively studied.

**Discussion:** The end-functionalized diblock copolymer (ZnPor-PAzo)-PNIPAM exhibits obvious fluorescence and efficient photocatalytic activity for aqueous MB under visible light.

## KEYWORDS

zinc porphyrin, diblock copolymer, fluorescence, cis/trans isomerization, photocatalytic activity, thermosensitive property, atom transfer radical polymerization

## 1 Introduction

The basic framework of porphyrins and their derivatives comprises four pyrrolic subunits that are linked by four methyne bridges. Owing to their conjugated macrocyclic structures, porphyrins possess excellent photochemical and photophysical characteristics (Liang et al., 2021). Therefore, porphyrins and their derivatives have widespread

applications, including CO<sub>2</sub>-reducing agents (Miyaji and Amao, 2021), light-harvesting materials (Zhang et al., 2003), pharmaceutical biomaterials (Panagiotakis et al., 2022), and photocatalysts (Kechich et al., 2021). However, porphyrins are prone to aggregation and insoluble in water. Therefore, they fail to exhibit photochemical activity in biological environments (Hone et al., 2002). Considering the abovementioned limitations, researchers have attempted to combine porphyrins with hydrophilic polymers or micelles (Ren et al., 2011; Tse et al., 2019). In our previous study, we prepared different end-functionalized poly (*N*-isopropylacrylamide) (PNIPAMs) via atom transfer-free radical polymerization (ATRP) and investigated their photodynamic therapy (Yang et al., 2014) and optical limiting properties (Qiu et al., 2013). Indeed, these end-functionalized polymers with porphyrin not only retained their photochemical and photophysical properties but also possessed water solubility and thermosensitivity owing to the introduction of hydrophilic chain segments. However, we observed that fluorescence intensity (Qiu et al., 2013; Yang et al., 2014) or reverse saturation absorption (Qiu et al., 2013) have a certain degree of diminished in intensity. This may be because the PNIPAM chain weakened the planar and conjugate properties of the porphyrin molecules. Therefore, developing functionalized polymers with multiple functional properties and efficient performance is vital.

To the best of our knowledge, azobenzene, a type of conjugated molecule, has widespread application owing to its *cis/trans* photoisomerization under specific wavelengths of ultraviolet (UV) light (Muraoka et al., 2006), including photoelectronic techniques (Tong et al., 2006), optical data storage (Åstrand et al., 2000), and liquid crystal displays (Han and Ichimura, 2001). Several scientific studies have reported the characteristics of azobenzene-porphyrins. The results showed that the electrochemical properties of the azobenzene-porphyrins are better than simple porphyrins (Hunter and Sarson, 1996; Tse et al., 2022). Furthermore, some researchers have synthesized azobenzene-containing block copolymers with PNIPAM chains and comprehensively elucidated their thermosensitive and photosensitive properties (Irie and Kungwachakun, 1992; Akiyama and Tamaoki, 2004). However, these multipolymers were obtained via traditional free radical copolymerization had higher polydispersity indexes (PDIs), which has bad effect on the properties of block copolymers (Ranganathan et al., 2008). Among

controlled/living radical polymerization methods, ATRP has been used to synthesize some multipolymers with controllable structures and more narrow molecular weight distribution (Wang and Matyjaszewski, 1995). So, in order to achieve the polymers with low PDIs, we used ATRP to synthesize the target polymers in the present study.

First, we used zinc (II) porphyrin (ZnPor)-Br as a specific initiator to synthesize poly (6-[4-(4-methoxyphenylazo)phenoxy] hexyl methacrylate) (ZnPor-PAzo) via ATRP. Then, ZnPor-PAzo was used as a macroinitiator and polymerized with NIPAM by ATRP to obtain the photochemical and thermoresponsive diblock biomaterial (ZnPor-PAzo)-PNIPAM. By taking advantage of the excellent conjugation of polyazobenzene and thermoresponsive property of PNIPAM, we hypothesized that fluorescence and other photoactivities of the biomaterial can be improved and some new functions can be endowed. Therefore, the biomaterial will display good performance for further applications in the photochemical and biomedical fields.

## 2 Materials and methods

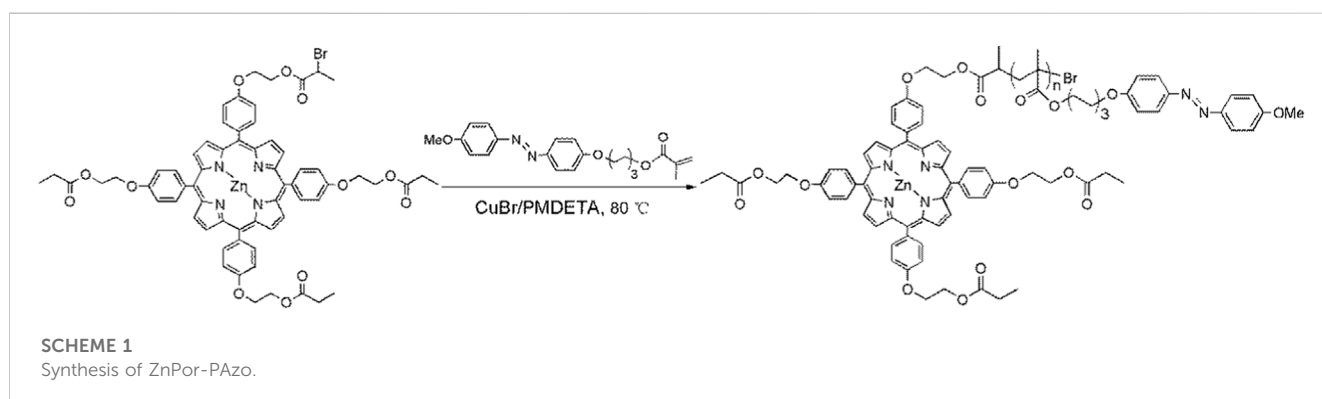
### 2.1 Cloud point testing

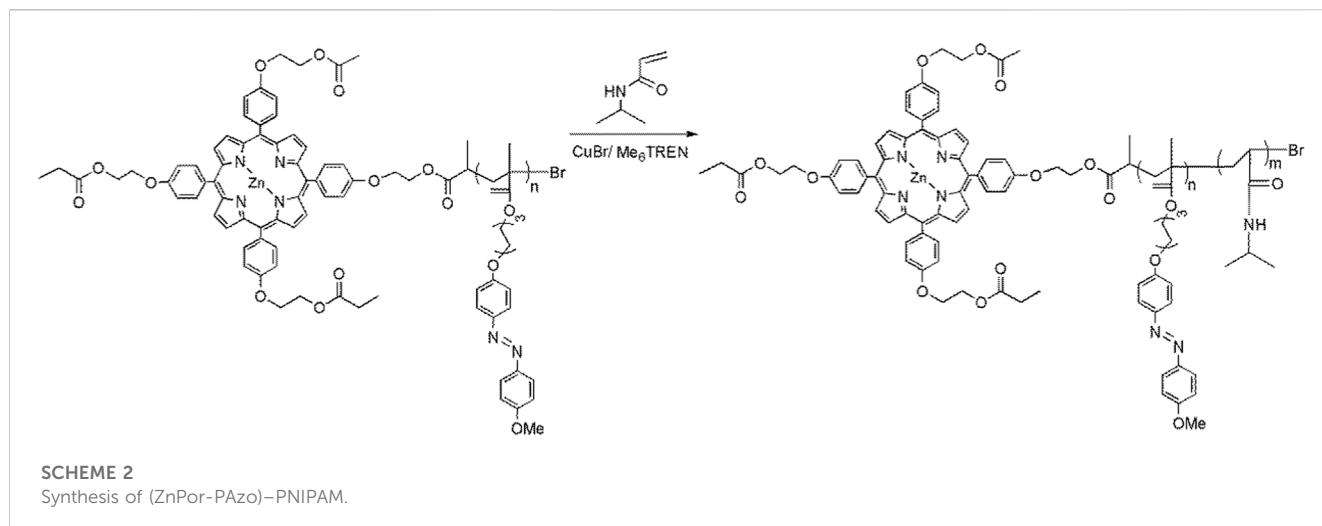
The samples were prepared as aqueous solutions (mass concentration of 2 mg/mL). These aqueous solutions were placed into the spectrophotometer cell. The samples were heated at 0.5°C/min, and the changes in the transmissivity of the aqueous solution were determined at a wavelength of 500 nm using a UV spectrophotometer.

### 2.2 Synthesis of ZnPor-PAzo via ATRP

The preparation procedures for ZnPor-OH, ZnPor-Br, and Azo are presented in the (Supplementary Schemes S1–S3) (Ringsdorf and Schmidt, 1984).

ZnPor-PAzo was synthesized as follows (Scheme 1). First, Azo (0.316 g, 0.8 mmol), CuBr (22 mg, 0.17 mmol), and PMDETA (40 μL, 0.17 mmol) were dissolved in anisole (2 mL) and subjected to three freeze-pump-thaw cycles under nitrogen protection. Second, ZnPor-Br (80 mg, 0.08 mmol) dissolved in anisole (2 mL) was added to the polymerization reactor to trigger





the polymerization reaction. The polymerization reaction was performed for 18 h at 70°C under nitrogen protection. Finally, the copper complex from the mixed product was removed via adsorption with aluminum oxide. The obtained products were dried for 12 h to obtain clean ZnPor-PAzo. Because azobenzene contains very strong hydrophobic groups, (ZnPor-PAzo)-PNIPAMs must have relatively long hydrophilic chain segments from the PNIPAM block and a suitable length of the hydrophobic chain segment from PAzo (<10 monomer units) for good water solubility (Ravi et al., 2005). In this study, the degree of polymerization of ZnPor-PAzo was 5 (50 mg, 25% yield,  $M_n = 3000$ , PDI = 1.04).

## 2.3 Synthesis of (ZnPor-PAzo)-PNIPAM

(ZnPor-PAzo)-PNIPAM was synthesized as follows (Scheme 2). NIPAM (1.79 g, 0.16 mol), CuBr (16 mg, 0.08 mmol), and Me<sub>6</sub>TREN (20 μL, 0.08 mmol) were dissolved in a suitable mixed solvent (DMF:water = 2:1, v/v). The solution was subjected to three freeze-pump-thaw cycles under nitrogen protection. Finally, ZnPor-PAzo ( $M_n = 3000$ , 0.02 mmol, 60 mg) dissolved in DMF (0.7 mL) was added to the polymerization reactor to induce the polymerization reaction. Under nitrogen protection, the polymerization reaction was performed for 3 days at 65°C. The mixed products were purified via dialysis (MWCO, 10,000) in DMF. Finally, the dialysis products were dried for 12 h to achieve clean (ZnPor-PAzo)-PNIPAM (210 mg, 45% yield,  $M_n = 21,000$ ,  $M_w/M_n = 1.23$ ).

## 2.4 Photocatalytic oxidative degradation test to evaluate the photocatalytic degradation of methylene blue by (ZnPor-PAzo)-PNIPAM

Hydrogen peroxide (H<sub>2</sub>O<sub>2</sub>) and (ZnPor-PAzo)-PNIPAM were added into a glass beaker containing an aqueous solution of 4 × 10<sup>-5</sup> mol/L MB; this comprised the photocatalytic degradation system. The solution was stirred well in a dark environment for 20 min. Thereafter, the photocatalytic degradation system was

exposed to a metal halide lamp (500 W) with an optical filter ( $\lambda > 450$  nm). During the degradation process, changes in the absorbance (665 nm) were detected at regular intervals using a UV/vis spectrophotometer to determine the photocatalytic degradation of MB in real-time. The degradation rate (D) of MB was calculated using the following formula:  $D = (A_0 - A)/A_0 \times 100\%$ , where  $A_0$  represents the original absorption strength (665 nm) and A represents the absorption strength at a specific time during testing.

## 3 Results and discussion

### 3.1 Synthesis and characterization of (ZnPor-PAzo)-PNIPAM

(ZnPor-PAzo)-PNIPAM was prepared using two ATRP reactions (Baek et al., 2011). To obtain multipolymers, precursors with narrow molecular weight distributions must be synthesized via ATRP. In the first ATRP, ZnPor-Br was used as an initiator to polymerize ZnPor-PAzo in anisole at 80°C for 20 h. The  $M_n$  values of ZnPor-PAzo and (ZnPor-PAzo)-PNIPAM were determined using gel permeation chromatography (GPC), and the PDI was 1.04, suggesting that the sample had a narrow molecular weight distribution (Table 1). The obtained ZnPor-PAzo was then used as a macroinitiator to polymerize NIPAM to synthesize the final product [(ZnPor-PAzo)-PNIPAM]. By regulating the feeding ratio of ZnPor-PAzo to NIPAM, (ZnPor-PAzo)-PNIPAMs with different molecular weights were obtained. Table 1 presents a detailed description of the experimental conditions and physical data.

### 3.2 Fourier-transform infrared spectroscopy (FT-IR)

Supplementary Figures S7A,B illustrate the FT-IR spectra of ZnPor-PAzo and (ZnPor-PAzo)-PNIPAM, respectively. From Supplementary Figure S7A, the characteristic absorptions of PAzoMA could be clearly observed, as evidenced by the presence of a methyne stretching vibration ( $\nu_{C-H}$ ) at 3088 cm<sup>-1</sup>. Furthermore, the stretching vibrations of the azo group ( $\nu_{N=N}$ ) were observed at 1601 and

TABLE 1 Experimental data of the polymerization reaction and LCST of (ZnPor-PAzo)-PNIPAMs.

Samples	$[M]_0/[I]_0^a$	time <sup>d</sup>	$M_n(\text{GPC})^e$	$M_n(\text{NMR})^f$	$M_w/M_n^g$	Yield (%) <sup>h</sup>	Azo (wt%) <sup>i</sup>	LCST (°C) <sup>j</sup>
ZnPor-(PAzo) <sub>10</sub>	50 <sup>b</sup>	16	3000	3200	1.04	25	68	---
P1	200 <sup>c</sup>	48	14,000	15,300	1.19	48	26	---
P2	400 <sup>c</sup>	72	21,000	23,000	1.23	51	16	20
P3	600 <sup>c</sup>	96	35,000	37,900	1.25	56	9	23
P4	800 <sup>c</sup>	96	43,000	45,000	1.29	50	7.5	25
P5	1000 <sup>c</sup>	96	57,000	59,700	1.32	48	3.3	28

<sup>a</sup>Feed molar ratio of monomer  $[M]_0$  to initiator  $[I]_0$ .

<sup>b</sup>[ZnPor-Br]: [PMDETA]: [Cu(I)Br] = 1:2:2.

<sup>c</sup>[ZnPor-PAzo]: [Me<sub>6</sub>TREN]: [Cu(I)Br] = 1:3:3.

<sup>d</sup>Time of the polymerization reaction in h.

<sup>e</sup> $M_n(\text{GPC})$  of ZnPor-PAzo, and (ZnPor-PAzo)-PNIPAMs, as determined using gel permeation chromatography (GPC).

<sup>f</sup> $M_n(\text{NMR})$  was determined using <sup>1</sup>H NMR, spectroscopy.

<sup>g</sup> $M_w/M_n$  of the samples prepared for GPC.

<sup>h</sup>Yield of (ZnPor-PAzo)-PNIPAMs.

<sup>i</sup>Proportion of ZnPor-PAzo, in (ZnPor-PAzo)-PNIPAMs.

<sup>j</sup>was measured using a UV/vis spectrophotometer.

1581 cm<sup>-1</sup>, as demonstrated in Supplementary Figure S7A), which belong to the characteristic infrared group frequency of ZnPor-PAzo.

Supplementary Figure S7B shows FT-IR absorption spectra of PAzoMA-b-PNIPAM, there are more new characteristic absorptions than just the peaks belonging to PAzoMA. The strong absorbance at 3304 cm<sup>-1</sup> was assigned to the stretching vibration ( $\nu_{\text{N-H}}$ ) of acylamino group and the characteristic absorption peaks originated from amide group were observed at 1650 cm<sup>-1</sup> ( $\nu_{\text{C=O}}$ ) and 1550 cm<sup>-1</sup> ( $\delta_{\text{N-H}}$ ).

### 3.3 Proton nuclear magnetic resonance (<sup>1</sup>H NMR) studies

Supplementary Figure S8B illustrates the <sup>1</sup>H NMR spectrum of ZnPor-PAzo. In contrast to the NMR spectrum of ZnPor-Br in Supplementary Figure S1A, the spectrum of ZnPor-PAzo displayed the consistent characteristic peaks belonging to ZnPor-Br at 8.77 and 8.11; the major characteristic peaks of protons belonging to PAzo were observed at 7.81, 6.91, 3.67, 1.37, and 1.30 ppm. Supplementary Figure S8A displays the <sup>1</sup>H NMR spectrum of (ZnPor-PAzo)-PNIPAM. Several new proton peaks appeared at 6.31, 5.53, 4.22, 1.64, and 1.35 ppm. These characteristic signals belong to the repeat units of NIPAM. In summary, the experimental results of FT-IR and <sup>1</sup>H NMR suggest the successful synthesis of end-functionalized ZnPor-PAzo and (ZnPor-PAzo)-PNIPAM via continuous ATRPs. In addition, the molecular weight of macroinitiator ZnPor-PAzo is obtained by <sup>1</sup>H NMR, so the molecular weight of (ZnPor-PAzo)-PNIPAM can be acquired by calculating the integral area of peaks to methylene (f + g') of ZnPor-PAzo and methyne (n) of (ZnPor-PAzo)-PNIPAM (Table 1). Furthermore, the  $M_n(\text{GPC})$  of polymers are higher than its  $M_n(\text{NMR})$ , it is because that the molecular weights obtained from GPC using polystyrene standards are a little high.

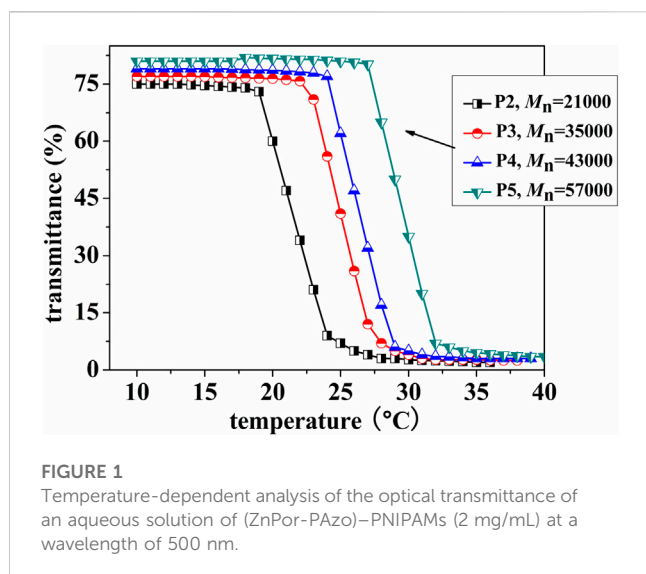
### 3.4 GPC studies

After a series of purifications, we used the Waters e2695 GPC system (with polystyrene as the standard) to determine the  $M_n$

values of ZnPor-PAzo and (ZnPor-PAzo)-PNIPAM. Table 1 presents the test results. Supplementary Figure S9 illustrates the GPC traces. A smooth and relatively symmetric curve with only one prominent peak was observed; this indicates that ZnPor-PAzo and (ZnPor-PAzo)-PNIPAM are pure and free of any small molecule such as the initiator, monomer or other byproducts residues in the final product. Notably, the peaks of the products were relatively narrow, and the PDI ( $M_w/M_n$ ) was 1.19–1.32, suggesting that the polymerization reactions were conducted in a controlled manner.

### 3.5 Temperature-sensitive characteristics of (ZnPor-PAzo)-PNIPAMs

To investigate the temperature-sensitive characteristics of (ZnPor-PAzo)-PNIPAMs, the lower critical solution temperature (LCST) was determined based on the optical transmissivity of (ZnPor-PAzo)-PNIPAM using the UVmini-1240 spectrophotometer (Shimadzu). Figure 1 shows the temperature-dependent analysis of the optical transmissivity of an aqueous solution of (ZnPor-PAzo)-PNIPAM at a wavelength of 500 nm. In the first stage, there was no marked variation in optical transmissivity with increasing temperature. This experimental phenomenon indicates that the temperature at this stage is below the LCST and that the hydrogen bond between the water molecule and amino group plays a prominent role; therefore, they are highly soluble in water. However, as the temperature increased, the powerful associative interaction of hydrophilic isopropyl inhibited the formation of intermolecular hydrogen bonds; as a result, the powerful repulsion arising from the hydrophobic groups led to the formation of large aggregates; the solution gradually became turbid when the temperature exceeds the LCST. In this experiment, the temperature at which the transmittance of (ZnPor-PAzo)-PNIPAM decreased by >10% was defined as the LCST at 500 nm. The results are listed in Table 1. As predicted, the results of the LCST experiment agreed with the finding that hydrophobic groups decrease the LCST of PNIPAM. The LCST of (ZnPor-PAzo)-PNIPAMs were lower than that of the homopolymer NIPAM, and the (ZnPor-PAzo)-PNIPAMs with



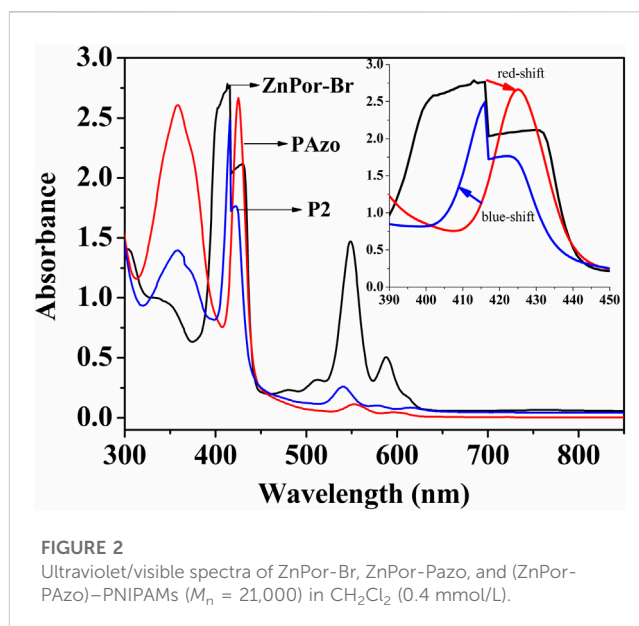
the  $M_{n(NMR)}$  of 15,300 cannot show the thermo-responsive property owing to the critical effect of the hydrophobic grouping ZnPor-PAzo (Xia et al., 2006). Furthermore, the LCST of (ZnPor-PAzo)-PNIPAMs gradually increased with an increase in  $M_n$ . The primary reason for this is that the effect of the hydrophilic groups on the properties of (ZnPor-PAzo)-PNIPAMs correspondingly increased.”

### 3.6 Photoresponsive property of (ZnPor-PAzo)-PNIPAMs

Figure 2 intuitively displays the UV/vis spectra of ZnPor-Br, PAzoMA, and (ZnPor-PAzo)-PNIPAMs in the form of a superposition. The B- and Q-bands of ZnPor-Br were located at 415 and 545–590 nm, respectively; this finding is consistent with that of similar metalloporphyrin derivatives (Papkovsky and O’riordan, 2005). Meanwhile, the UV/vis absorption spectrum of ZnPor-PAzo revealed the characteristic band of azobenzene at approximately 360 nm and the B and Q-bands at 424 and 545–590 nm, respectively. Compared with ZnPor-Br, the B- and Q-bands of ZnPor-PAzo exhibited a bathochromic shift. This is because the organic conjugated groups (azobenzene) replace the electron-withdrawing groups (-Br), thereby decreasing the lowest empty orbital and increasing the highest orbital energy levels simultaneously; therefore the B- and Q-bands exhibit a redshift phenomenon. Moreover, we observed another interesting phenomenon: compared with ZnPor-PAzo the B- and Q-bands of (ZnPor-PAzo)-PNIPAMs exhibited a blue shift, which was caused by the severe steric hindrance effect of the polymer segments.

### 3.7 Cis/trans isomerization of (ZnPor-PAzo)-PNIPAMs under UV/vis light irradiation

The cis/trans isomerization of (ZnPor-PAzo)-PNIPAM was determined in aqueous solutions after UV exposure (365 nm, 8 W). Figure 3 illustrates the changes in the UV/vis absorption



spectra at different UV illumination times. (ZnPor-PAzo)-PNIPAM exhibited two absorption bands at approximately 360 and 470 nm; these bands belonged to the  $\pi-\pi^*$  and  $n-\pi^*$  transition bands of trans- and cis-azobenzene, respectively. With an increase in UV irradiation time, the intensity of the  $\pi-\pi^*$  transition band at approximately 360 nm gradually became weak; on the other hand, the  $n-\pi^*$  transition band at approximately 470 nm was gradually enhanced. The photostationary state was achieved at 365 nm after irradiation for 90 min. When the (ZnPor-PAzo)-PNIPAM was exposed to visible light (450 nm) or dark conditions for approximately 60 min, the trans-azobenzene content of (ZnPor-PAzo)-PNIPAM was completely recovered. Furthermore, a repetitive cycle experiment of the cis/trans isomerization of (ZnPor-PAzo)-PNIPAM was performed; the results are illustrated in Figure 3A. After irradiation for 90 min at 365 nm, the intensity of the  $n-\pi^*$  transition band at approximately 470 nm was the highest and that of the  $\pi-\pi^*$  transition band at approximately 360 nm was the lowest. In contrast, after light irradiation for 60 min at 450 nm, the intensity of the  $n-\pi^*$  transition band was the lowest, whereas that of the  $\pi-\pi^*$  transition band was the highest. These steps were repeated seven times. The cis/trans isomerization was stable and did not delay the reaction time. Taken together, the above experimental results suggest that (ZnPor-PAzo)-PNIPAM not only undergoes cis/trans isomerization but also exhibits favorable repeatability, which is vital for practical applications.

### 3.8 Fluorescence spectrum results

Several related experimental studies have reported that porphyrins and their derivatives can be used as fluorescent dyes (Fang et al., 2008; Tao et al., 2011). Therefore, we discussed and compared the fluorescence properties of ZnPor-Br, ZnPor-PAzo, and (ZnPor-PAzo)-PNIPAM. Figure 4A illustrates the fluorescence spectra of the samples. The emission maximum was observed at



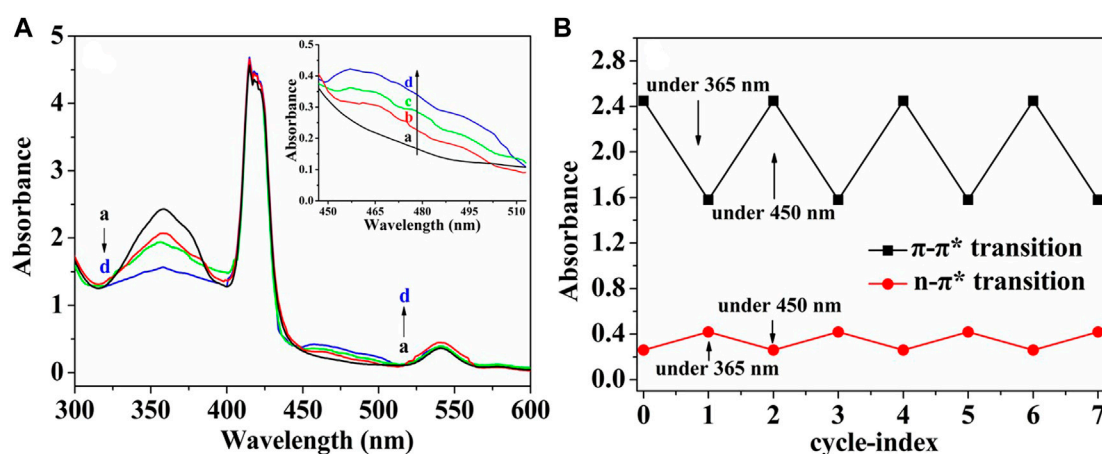


FIGURE 3

(A) Spectral changes in the aqueous solution of (ZnPor-PAzo)-PNIPAM ( $M_n = 21,000$ ) under ultraviolet UV light (365 nm, 8 W). Exposure time: (a) 0 min, (b) 20 min, (c) 50 min, and (d) 90 min. (B) Repetitive cycle experiment of the cis/trans isomerization of (ZnPor-PAzo)-PNIPAM ( $M_n = 21,000$ ). The biomaterial was UV irradiated for 90 min and exposed to visible light (450 nm) for 60 min for one operating cycle.

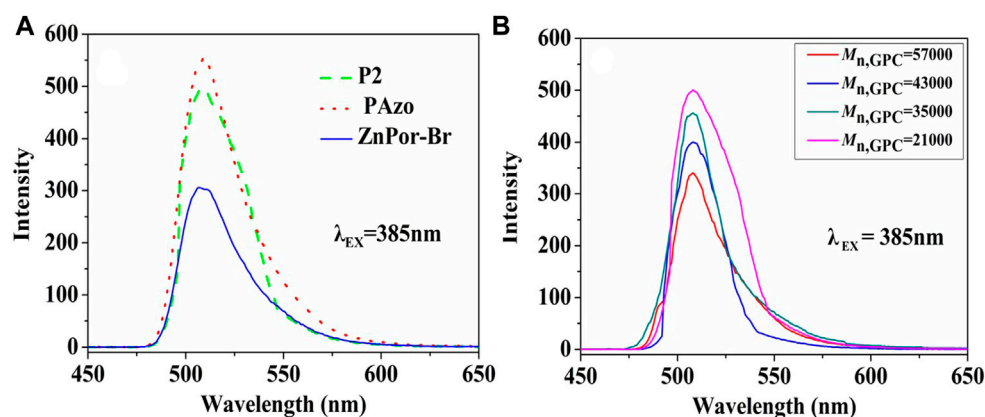


FIGURE 4

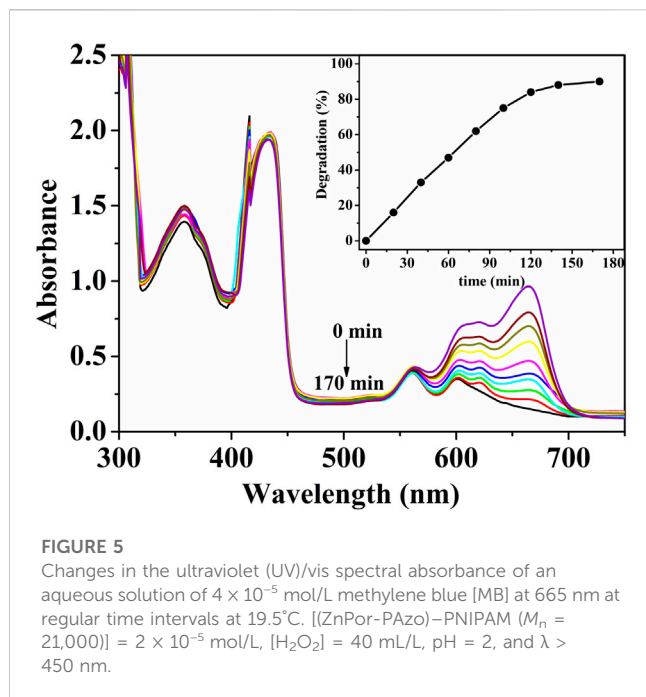
(A) Fluorescence spectra of ZnPor-Br, ZnPor-PAzo, and P2 [(ZnPor-PAzo)-PNIPAM,  $M_n = 21,000$ ] at a concentration of  $2 \times 10^{-5}$  mol/L in DMF. Analysis was performed using the Shimadzu RF-5301PC fluorescence spectrophotometer (B) Changes in the fluorescence intensity of (ZnPor-PAzo)-PNIPAMs with different  $M_n$ .

approximately 507 nm at an excitation wavelength of 385 nm. However, the fluorescence intensities of ZnPor-Br, ZnPor-PAzo, and (ZnPor-PAzo)-PNIPAM were significantly different. The fluorescence intensity of ZnPor-PAzo was much stronger than that of ZnPor-Br. This may be because of the following two points. First, ZnPor-PAzo has a noticeable absorption peak between 335 and 390 nm, which has some degree of overlap with the PLE of ZnPor-PAzo (385 nm), and ZnPor-PAzo achieves more energy because of energy transmission. Second, the addition of azobenzene may considerably enhance the  $\pi$ -electronic conjugation. In contrast, the fluorescence intensity of (ZnPor-PAzo)-PNIPAM was weaker than that of ZnPor-PAzo to some extent. This could be because the  $\pi-\pi$  conjugation was weakened by the severe steric hindrance effect of the polymer segments. In addition, we studied the effect of  $M_n$  on the fluorescence

intensity of (ZnPor-PAzo)-PNIPAM at an excitation wavelength of 385 nm. As shown in Figure 4B, the fluorescence intensity of (ZnPor-PAzo)-PNIPAM slowly decayed with an increase in  $M_n$ , without significant fluorescence quenching after polymerization. (Qiu et al., 2014)."

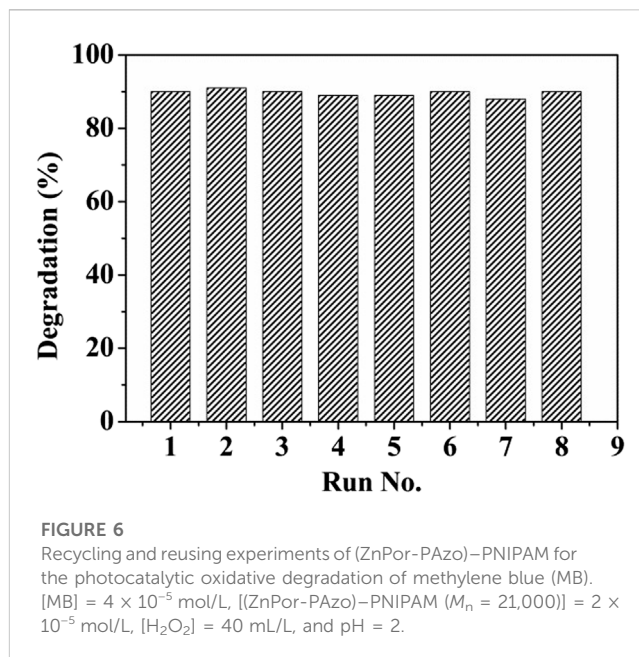
### 3.9 Photocatalytic performance of (ZnPor-PAzo)-PNIPAM on MB

In this study, the photocatalytic activity of (ZnPor-PAzo)-PNIPAM was investigated by performing photocatalytic experiments in which MB was exposed to visible light. After a series of photocatalytic experiments, we verified that the experimental conditions and factors influencing the photocatalytic



activity of (ZnPor-PAzo)-PNIPAM were consistent with those reported in our previous study (Faustova et al., 2020). The experimental results are shown in Figure 5; the characteristic peak of MB at 665 nm rapidly decreased with increasing reaction time and nearly disappeared after 170 min. In other words, MB concentration gradually decreased as the earlier catalytic degradation reaction progressed; the degradation rate reached approximately 90%. The above experimental results suggest that (ZnPor-PAzo)-PNIPAM exerts an excited photocatalytic degradation effect on MB under visible light irradiation. Furthermore, the peaks of (ZnPor-PAzo)-PNIPAM at 360 and 420 nm did not change as degradation time increased; this suggests that (ZnPor-PAzo)-PNIPAM maintains structural stability during catalytic degradation.

Finally, the reusability and stability of (ZnPor-PAzo)-PNIPAM were tested. After the catalytic degradation of MB with the fresh (ZnPor-PAzo)-PNIPAM catalyst, the used (ZnPor-PAzo)-PNIPAM can be recycled via a simple and easy filtration process owing to its thermoresponsive properties. First, the temperature was increased above the LCST; (ZnPor-PAzo)-PNIPAM agglomerated to form solid particles in water. The precipitated solid particles were then filtered and washed five times with deionized water. Finally, the solid particles were dried at 60°C in vacuum for 10 h. Recycled (ZnPor-PAzo)-PNIPAM was added again to the newly prepared MB solution, and a second catalytic degradation and recovery experiment was performed under invariable experimental conditions. Recycling tests were performed eight times. The results of the tests are displayed in Figure 6. Notably, the degradation rate of MB basically remained at approximately 90%. The abovementioned experimental results suggest that (ZnPor-PAzo)-PNIPAM exhibits excellent photocatalytic degradation ability and can be easily recycled without secondary pollution.



## 4 Conclusion

By the ATRP reactions, we have successfully fabricated a series of efficient and green photocatalytic degradation agents [(ZnPor-PAzo)-PNIPAM] for MB under visible light. In addition, (ZnPor-PAzo)-PNIPAM can be recycled several times to maintain its photocatalytic degradation characteristics. The thermoresponsive diblock copolymers (ZnPor-PAzo)-PNIPAM not only exhibited representative cis/trans isomerism when exposed to sufficient UV light but also had significantly enhanced fluorescence intensity in DMF. Therefore, these (ZnPor-PAzo)-PNIPAMs which have good temperature-sensitive water solubility and fluorescence characteristic expected to have potential application value in the field of biomolecular recognition.

## Data availability statement

The original contributions presented in the study are included in the article/Supplementary Material, further inquiries can be directed to the corresponding author.

## Author contributions

NQ: Data curation, Investigation, Writing—original draft, Writing—review and editing. XP: Methodology, Supervision, Writing—original draft. RH: Formal Analysis, Methodology, Writing—review and editing. ZH: Investigation, Methodology, Writing—review and editing, Formal Analysis, Funding acquisition, Writing—original draft.

## Funding

The author(s) declare financial support was received for the research, authorship, and/or publication of this article. This research was funded by the research and development and industrialization of green environmental porphyrin-based photocatalysis agent (881226), the Talent Introduction Project of Anhui Science and Technology University (200110), the Major Foundation of Education Department of Anhui Province (2022AH051655), the Anhui Young Scholars Project (830523), and the Foundation of Anhui College Students' Innovation and Entrepreneurship (grant number 20211087903).

## Acknowledgments

The authors are grateful to the Anhui Science and Technology University, our colleague and all reviewers of this article for their comments and suggestions. We would like to thank Editage ([www.editage.com](http://www.editage.com)) for English language editing.

## References

- Akiyama, H., and Tamaoki, N. (2004). Polymers derived from N-isopropylacrylamide and azobenzene-containing acrylamides: photoresponsive affinity to water. *J. Polym. Sci. A Polym. Chem.* 42, 5200–5214. doi:10.1002/pola.20307
- Åstrand, P., Ramanujam, P. S., Hvilsted, S., Bak, K. L., and Sauer, S. P. A. (2000). *Ab initio* calculation of the electronic spectrum of azobenzene dyes and its impact on the design of optical data storage materials. *J. Am. Chem. Soc.* 122, 3482–3487. doi:10.1021/ja993154r
- Baek, K., Lee, S.-H., and Hwang, S. S. (2011). Synthesis of amphiphilic star block copolymer with photosensitive core by ATRP. *Macromol. Res.* 19, 461–467. doi:10.1007/s13233-011-0508-6
- Fang, Z., Pu, K.-Y., and Liu, B. (2008). Asymmetric fluorescence quenching of dual-emissive porphyrin-containing conjugated polyelectrolytes for naked-eye mercury ion detection. *Macromolecules* 41 (22), 8380–8387. doi:10.1021/ma801874z
- Faustova, M., Nikolskaya, E., Sokol, M., Fomicheva, M., Petrov, R., and Yabbarov, N. (2020). Metalloporphyrins in medicine: from history to Recent trends. *ACS Appl. Bio Mater.* 3, 8146–8171. doi:10.1021/acsbm.0c00941
- Han, M., and Ichimura, K. (2001). Tilt orientation of *p*-methoxyazobenzene side chains in liquid crystalline polymer films by irradiation with nonpolarized light. *Macromolecules* 34, 82–89. doi:10.1021/ma0008239
- Hone, D. C., Walker, P. I., Evans-Gowing, R., FitzGerald, S., Beeby, A., Chambrier, I., et al. (2002). Generation of cytotoxic singlet oxygen via phthalocyanine-stabilized gold nanoparticles: a potential delivery vehicle for photodynamic therapy. *Langmuir* 18, 2985–2987. doi:10.1021/la0256230
- Hunter, C. A., and Sarson, L. D. (1996). Azobenzene-porphyrins. *Tetrahedron Lett.* 37, 699–702. doi:10.1016/0040-4039(95)02246-5
- Irie, M., and Kungwachakun, D. (1992). Stimuli-responsive polymers. Photostimulated reversible phase separation of aqueous solutions of poly(N-isopropylacrylamide) with pendant azobenzene groups. *Proc. Jpn. Acad. Ser. B* 68, 127–132. doi:10.2183/pjab.68.127
- Kechich, A., Soury, R., Jabli, M., Alenezi, K. M., Philouze, C., and Nasri, H. (2021). Synthesis of novel bis(cyano) meso-tetraphenylporphyrinato-chromium(III), [K(2 2 2)] [CrIII(TPP)(CN)2] 2.(C7H6O2) (III), and (Chloro) meso-tetraphenylporphyrinato-chromium(III), [CrIII(TPP)Cl] (II): spectroscopic, physico-chemical, and decolorization properties. *Inorg. Chem. Commun.* 128, 1–10. doi:10.1016/j.inoche.2021.108588
- Liang, Z., Wang, H. Y., Zheng, H., Zhang, W., and Cao, R. (2021). Porphyrin-based frameworks for oxygen electrocatalysis and catalytic reduction of carbon dioxide. *Chem. Soc. Rev.* 50, 2540–2581. doi:10.1039/d0cs01482f
- Miyaji, A., and Amao, Y. (2021). Visible-light-driven reduction of CO<sub>2</sub> to formate by a water-soluble zinc porphyrin and formate dehydrogenase system with electron-

## Conflict of interest

The authors declare that the research was conducted in the absence of any commercial or financial relationships that could be construed as a potential conflict of interest.

## Publisher's note

All claims expressed in this article are solely those of the authors and do not necessarily represent those of their affiliated organizations, or those of the publisher, the editors and the reviewers. Any product that may be evaluated in this article, or claim that may be made by its manufacturer, is not guaranteed or endorsed by the publisher.

## Supplementary material

The Supplementary Material for this article can be found online at: <https://www.frontiersin.org/articles/10.3389/fbioe.2023.1268458/full#supplementary-material>

mediated amino and carbamoyl group-modified viologen. *New J. Chem.* 45, 5780–5790. doi:10.1039/D1NJ00889G

Muraoka, T., Kinbara, K., and Aida, T. (2006). Mechanical twisting of a guest by a photoresponsive host. *Nature* 440, 512–515. doi:10.1038/nature04635

Panagiotakis, S., Mavroidi, B., Athanopoulos, A., Charalambidis, G., Coutsolelos, A. G., Paravatou-Petsotas, M., et al. (2022). Unsymmetrical, monocarboxyalkyl meso-arylporphyrins in the photokilling of breast cancer cells using permethyl- $\beta$ -cyclodextrin as sequesterant and cell uptake modulator. *Carbohydr. Polym.* 275, 118666. doi:10.1016/j.carbpol.2021.118666

Papkovsky, D. B., and O'Riordan, T. C. (2005). Emerging applications of phosphorescent metalloporphyrins. *J. Fluoresc.* 15, 569–584. doi:10.1007/s10895-005-2830-x

Qiu, N. N., Li, Y. H., Han, S. L., Satoh, T., Kakuchi, T., and Duan, Q. (2014). Synthesis of end-functionalized poly(N-isopropyl acrylamide) with zinc porphyrin and its photocatalytic activity under visible light. *J. Appl. Polym. Sci.* 131. doi:10.1002/app.40523

Qiu, N., Liu, D., Han, S., He, X., Cui, G., and Duan, Q. (2013). Synthesis of the end-functionalized polymethyl methacrylate incorporated with an asymmetrical porphyrin group via atom transfer radical polymerization and investigation on the third-order nonlinear optical properties. *J. Photochem. Photobiol. A Chem.* 272, 65–72. doi:10.1016/j.jphotochem.2013.08.016

Ranganathan, K., Deng, R., Kainthan, R. K., Wu, C., Brooks, D. E., and Kizhakkedathu, J. N. (2008). Synthesis of thermoresponsive mixed arm star polymers by combination of RAFT and ATRP from a multifunctional core and its self-assembly in water. *Macromolecules* 41, 4226–4234. doi:10.1021/ma800094d

Ravi, P., Sin, S. L., Gan, L. H., Gan, Y. Y., Tam, K. C., Xia, X. L., et al. (2005). New water soluble azobenzene-containing diblock copolymers: synthesis and aggregation behavior. *Polymer* 46, 137–146. doi:10.1016/j.polymer.2004.11.009

Ren, T., Wang, A., Yuan, W., Li, L., and Feng, Y. (2011). Synthesis, self-assembly, fluorescence, and thermosensitive properties of star-shaped amphiphilic copolymers with porphyrin core. *J. Polym. Sci. A Polym. Chem.* 49, 2303–2313. doi:10.1002/pola.24665

Ringsdorf, H., and Schmidt, H. W. (1984). Electro-optical effects of azo dye containing liquid crystalline copolymers. *Makromol. Chem.* 185, 1327–1334. doi:10.1002/macp.1984.021850706

Tao, Y., Xu, Q., Li, N., Lu, J., Wang, L., and Xia, X. (2011). Synthesis and photoluminescent property of star polymers with carbazole pendent and a zinc porphyrin core by ATRP. *Polymer* 52, 4261–4267. doi:10.1016/j.polymer.2011.07.025



Tong, X., Wang, G., and Zhao, Y. (2006). Photochemical phase transition versus photochemical phase separation. *J. Am. Chem. Soc.* 128, 8746–8747. doi:10.1021/ja063244d

Tse, H., Yeung, C. S., Lau, C. Y., Cheung, M. Y., Guan, J., Islam, M. K., et al. (2022). One-pot synthesis to prepare lignin/photoacid nanohybrids for multifunctional biosensors and photo-triggered singlet oxygen generation. *Green Chem.* 24, 2904–2918. doi:10.1039/D2GC00196A

Tse, H. Y., Cheng, S. C., Yeung, C. S., Lau, C. Y., Wong, W. H., Dong, C., et al. (2019). Development of a waste-derived lignin-porphyrin bio-polymer with enhanced photoluminescence at high water fraction with wide pH range and heavy metal sensitivity investigations. *Green Chem.* 21, 1319–1329. doi:10.1039/C8GC02904K

Wang, J. S., and Matyjaszewski, K. (1995). Controlled/living radical polymerization. atom transfer radical polymerization in the presence of transition-metal complexes. *J. Am. Chem. Soc.* 117, 5614–5615. doi:10.1021/ja00125a035

Xia, Y., Burke, N. A. D., and Stöver, H. D. H. (2006). End group effect on the thermal response of narrow-disperse poly(N-isopropylacrylamide) prepared by atom transfer radical polymerization. *Macromolecules* 39, 2275–2283. doi:10.1021/ma0519617

Yang, Y., Li, Y. H., Qiu, N. N., Cui, G. H., Satoh, T., and Duan, Q. (2014). Synthesis and characterization of aminoporphyrin-end-functionalized poly(N-isopropylacrylamide) with photodynamic and thermoresponsive effects. *Chem. Asian J.* 9, 1379–1387. doi:10.1002/asia.201301513

Zhang, G. D., Nishiyama, N., Harada, A., Jiang, D. L., Aida, T., and Kataoka, K. (2003). pH-sensitive assembly of light-harvesting dendrimer zinc porphyrin bearing peripheral groups of primary amine with poly(ethylene glycol)-b-poly(aspartic acid) in aqueous solution. *Macromolecules* 36, 1304–1309. doi:10.1021/ma025735y